



ELSEVIER

Nuclear Physics A682 (2001) 28c–34c

www.elsevier.nl/locate/npe

Rotational bands near ^{56}Ni

W. Reviol^a, D.G. Sarantites^a, R.J. Charity^a, V. Tomov^a, D. Rudolph^b, R.M. Clark^c, M. Cromaz^a, P. Fallon^a, A.O. Macchiavelli^c, M.P. Carpenter^d, D. Seweryniak^d, and J. Dobaczewski^e

^aChemistry Department, Washington University, St. Louis, MO 63132, USA

^bDepartment of Physics, Lund University, S-22100 Lund, Sweden

^cNuclear Science Division, Lawrence Berkeley National Lab., Berkeley, CA 94720, USA

^dPhysics Division, Argonne National Laboratory, Argonne, IL 60439, USA

^eInstitute of Theoretical Physics, Warsaw University, PL-00681, Warsaw, Poland

Rotational bands have been found in ^{57}Co and ^{57}Ni , using Gammasphere in conjunction with the Microball and 30 neutron detectors. The bands in ^{57}Co , extending the mass 60 region of deformation down to $Z = 27$, are signature partner sequences. The quadrupole moments and dynamic moments of inertia of the new bands in both nuclei are similar to those of rotational sequences in the neighboring nuclei. The high-spin structure of ^{57}Co is compared with Skyrme Hartree-Fock calculations.

1. INTRODUCTION

Rotational bands associated with a highly deformed ($\beta_2 > 0.3$) or superdeformed ($\beta_2 > 0.5$) quadrupolar shape have been found in nuclei in the mass 60 region, specifically in the isotopic chains of Zn, Cu, and Ni (see *e.g.* Refs. [1–4]). Various model approaches explain the deformed configurations in this region by particle-hole excitations across the $N = Z = 28$ shell gap which involve the strongly deformation driving $N_0 = 4$ $g_{9/2}$ intruder orbital (see *e.g.* Refs. [4–6]). Throughout the whole region, these bands exhibit a drop in the dynamic moment of inertia, $\mathcal{J}^{(2)}$, with increasing rotational frequency, $\hbar\omega$. This characteristic feature of $\mathcal{J}^{(2)}$ is attributed to a so-called smooth band termination [2], implying configuration changes and a gradual loss of collectivity with $\hbar\omega$. However, despite the expected loss of collectivity the bands remain well-deformed over the entire spin range. In the present work, the picture of particle-hole excitations with significant intruder content across the shell closure is tested further by studying the rather light odd-mass nuclei, ^{57}Co and ^{57}Ni .

2. EXPERIMENT AND DATA REDUCTION

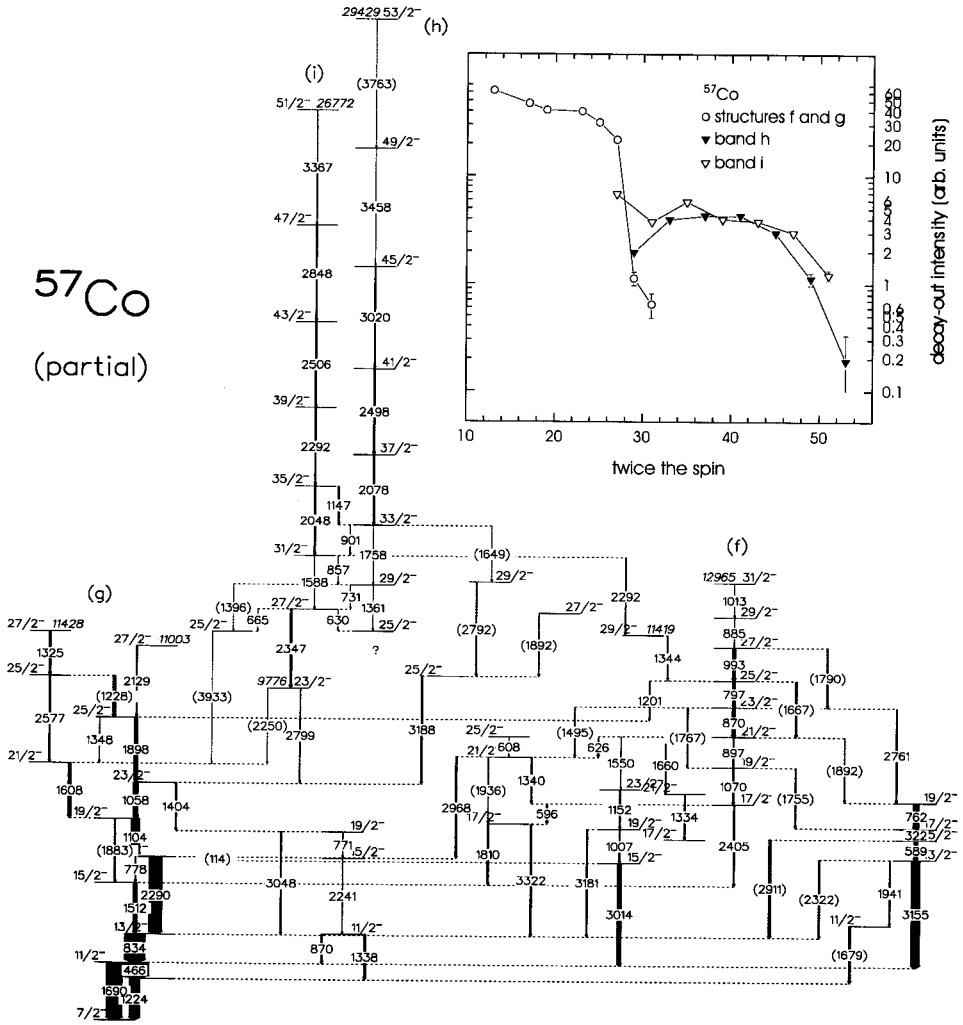
The experiment was carried out at the ATLAS facility at Argonne National Laboratory. The $^{32}\text{S} + ^{28}\text{Si} \rightarrow ^{60}\text{Zn}^*$ reaction at a beam energy of 130 MeV was used to produce fusion-

evaporation residues around ^{56}Ni at high spin. The target enriched to 99% in ^{28}Si had a surface density of 0.5 mg/cm^2 and was supported by a 1 mg/cm^2 Au layer facing the beam. The γ rays from the reaction were detected by the Gammasphere array [7], which contained 78 Ge detectors in BGO Compton-suppression shields. The hevimet collimators were removed to obtain γ -ray sum energy and fold information per event. A shell of 30 neutron detectors [8] was used for the first time in Gammasphere, replacing thirty Ge-BGO modules of the six most forward rings. The Neutron Shell served for the purpose of selecting one and two neutron evaporation channels, while the evaporated charged particles were detected with the 4π CsI-array Microball [9]. A total of about 700 million events were collected during two days of running time, with the condition that a minimum of two “clean” Ge detectors and a neutron detector fired in coincidence.

In the offline analysis, the γ -ray data were sorted according to individual exit channels by gating on the identified charged particles or neutrons or a combination of both. Contaminants in these gates resulting from particles which escaped detection were sharply reduced by applying the total energy plane selection method of Ref. [10]. The ^{57}Co and ^{57}Ni nuclei under consideration were populated in the 3p and 2pn channels, respectively. An efficiency for one neutron detection of $\sim 33\%$ was achieved, as inferred from the selection of the 2pn channel (and 3pn channel leading to ^{56}Co [11]). To sharpen the γ -ray spectra, a precise Doppler shift correction was performed: the velocity vector of the recoiling nucleus was reconstructed (taking into account the momentum vectors of the charged particles determined with the Microball and the detected neutrons) and a γ -ray energy dependent recoil velocity was applied. In the case of ^{57}Co and ^{57}Ni , a residual Doppler-shift analysis [12] was performed subsequently to obtain transition quadrupole moments for the level structures of interest.

3. RESULTS

Fig. 1 shows the main part of the new level scheme for ^{57}Co (some non-yrast states are omitted). The spin and parity assignments for the levels up to the first $19/2^-$ state are adopted from previous work [13]. The spins for the higher lying states are assigned on the basis of the γ -ray multipolarities obtained from a directional correlation (DCO) analysis. In addition, it is *assumed* that levels decaying predominantly to known negative-parity levels have themselves negative parity. The low spin level structure is very complex and probably reflects the many possibilities of single-particle excitations in this nucleus. However, above spin $25/2$ a band structure develops. The two high-spin $E2$ sequences labeled (h) and (i) are at the bottom interlinked by dipole transitions which are proposed to be of $M1$ type. The $E2$ sequences are viewed as signature partner bands. Their drop in $\mathcal{J}^{(2)}$ ($\propto 1/\Delta E_\gamma$) with spin resembles other band structures in the region. Fig. 2 shows sample coincidence spectra for the bands (h) and (i). These spectra are obtained from sums of coincidence gates placed on inband transitions. All band members and the interband transitions are labeled by their energies in keV. The spectra have in common that the same transitions between 731 and 1147 keV (dipoles) are present and cross-talk between both sequences occurs. Thus, they support the high-spin part of the level scheme.



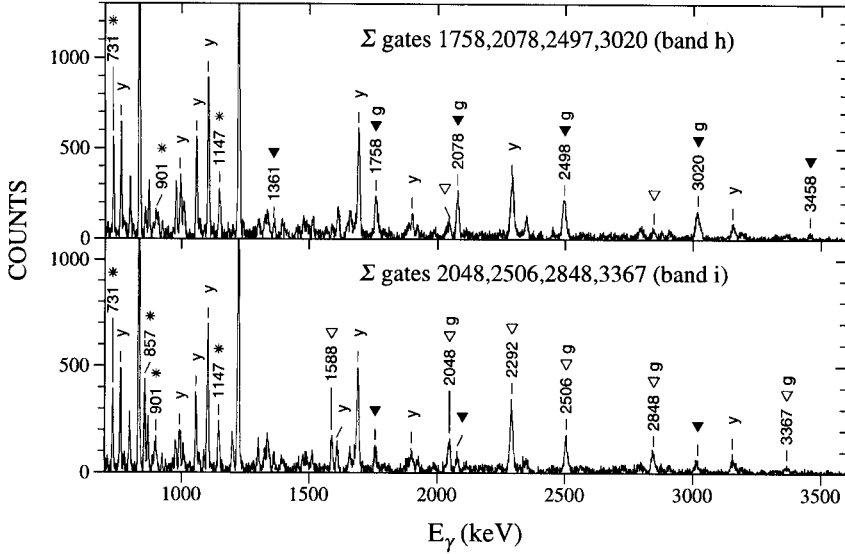


Figure 2. Coincidence spectra for the high spin band structure in ^{57}Co . Gating transitions are given in the figure and labeled by the symbol “g”. The transitions in the sequences (h) and (i) are highlighted by filled and open triangles, respectively, signature partner linking transitions by asterisks. The most intense γ rays and those labeled by “y” are yrast transitions between lower-lying states in ^{57}Co .

The decay intensity of the signature partner bands in ^{57}Co is spread over several pathways linking the bands with both the level structure (f) and (g). However, the observed linking transitions account for $\sim 80\%$ of the intensity of the bands. Notice also that the decay of the weakly populated $25/2^-$ “bandhead” state is not observed, as indicated in Fig. 1. It is important to ensure that in the present level scheme no significant linking transitions are missing and an independent check of the spin assignments is in order. The inset of Fig. 1 shows the intensity patterns of the yrast sequences over a large spin range. Indeed, the crossing of these patterns is supportive for the spin assignments. Furthermore, the possibility of a proton decay at the bottom of the ^{57}Co bands, similar to the case of ^{58}Cu [3], is unlikely since γ rays of ^{56}Fe (possible daughter nucleus) are absent in the spectra of interest. Therefore, the bands in ^{57}Co are considered to be fairly well linked to the low-spin part of the level scheme.

The rotational character of band (h) and (i) is inferred from their average transition quadrupole moments, Q_0 , obtained by using the thin-target Doppler-shift attenuation method [12]. Due to the high γ -ray energies the level lifetimes are short compared to the average time taken by the recoiling nuclei to traverse the target (~ 100 fs). The measured fractional Doppler-shifts, $F(\tau)$ vs. E_γ , for each band have been fitted by calculated $F(\tau)$ curves, using the side feeding model of Ref. [14], the measured intensity profiles of bands (h) and (i), and for the slowing down process in the target the stopping powers provided by

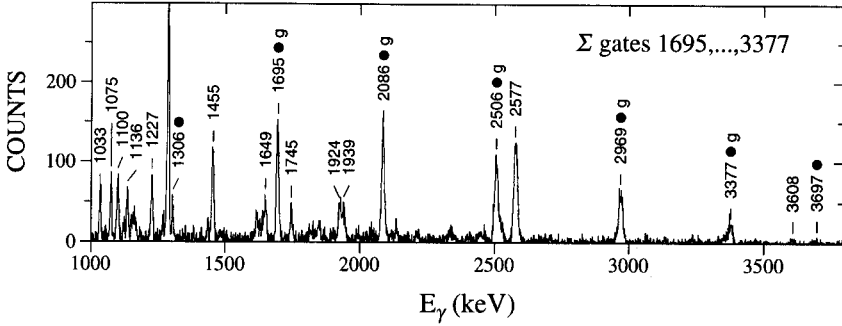


Figure 3. Sample coincidence spectrum for ^{57}Ni populated in the $(^{32}\text{S},2\text{pn})$ reaction. The transitions of the rotational band are highlighted (dots).

the code TRIM [15]. The results obtained from a χ^2 minimization for the free parameter are $Q_0 = 1.9_{-0.4}^{+0.6}$ eb and $1.95_{-0.5}^{+0.8}$ eb for band (h) and (i), respectively. The quoted errors represent a 1σ deviation from the best fit but exclude the systematic errors associated with the stopping powers which are smaller. The measured Q_0 values correspond to a quadrupole deformation $\beta_2 = 0.39$ or an even larger elongation if a non-axial shape with $\gamma > 0^\circ$ is assumed. That is, the bands in ^{57}Co represent a highly deformed shape of the nucleus.

The present data have also revealed a rotational band in ^{57}Ni . This $E2$ sequence consists of seven transitions with the respective energies of 1306, 1695, 2086, 2506, 2969, 3377, and 3697 keV and extends the level scheme of ^{57}Ni [16] to significantly higher spin ($> 22\hbar$). The lowest lying band member (1306 keV) is *tentatively* assigned as a $23/2 \rightarrow 19/2$ transition. Fig. 3 shows a sample spectrum for ^{57}Ni obtained from a sum of coincidence gates. Known yrast and near-yrast transitions (below spin $21/2$) are labeled by their energies in keV only. The members of the newly observed band are highlighted by dots. Using the thin-target DSAM method, an average quadrupole moment has been obtained for the band in ^{57}Ni as well. The measured value $Q_0 = 2.3_{-0.7}^{+0.9}$ eb corresponds to a deformation $\beta_2 = 0.45$ (for $\gamma = 0^\circ$), which is perhaps comparable with the feature of a superdeformed band in the region, *e.g.* that in ^{56}Ni [3].

4. DISCUSSION AND CONCLUSIONS

The properties of the new bands in ^{57}Co are compared with results of Cranked Hartree-Fock calculations using the Skyrme interaction SLy4 [17]. The configurations are described by the notation 4^n4^p , where n and p are the numbers of occupied $N_0 = 4$ unique parity routhians. For example, the doubly magic superdeformed configuration in ^{60}Zn can be labeled 4^24^2 (no hole state). Briefly, the configuration assignment proposed for ^{57}Co rests on (i) parity considerations, (ii) quadrupole moments, (iii) configuration crossings judged by the $\mathcal{J}^{(2)}$ vs. $\hbar\omega$ behavior, and (iv) comparisons of the spin sequences of both signatures with the expected band terminating spins. Since the bands in ^{57}Co have most likely negative parity, only intruder configurations of the 4^24^0 type (one proton hole) and the 4^14^1

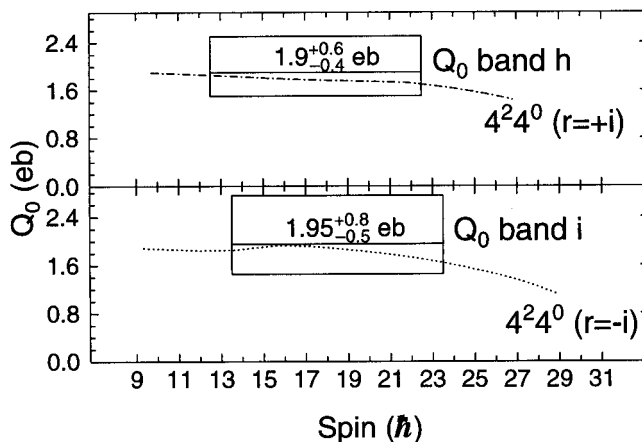


Figure 4. Comparison between measured and calculated quadrupole moments for the bands in ^{57}Co . The boxes represent the average Q_0 values (with error) measured in a certain spin range (*cf.* Section 3).

type (one additional neutron in a negative-parity orbital) are possible. Other negative-parity configurations without intruder content are ruled out by the large quadrupole moment measured. However, among these two options the $4^2 4^0$ configuration matches the $\mathcal{J}^{(2)}$ moments and spin sequences best. Interestingly, the first crossing between the proton routhians (at $\hbar\omega \sim 1$ MeV) involves the $K = 5/2^- f_{7/2}$ prolate state, an orbital with a small degree of signature splitting. This explains why the band structure is observed in both signatures.

The good agreement between experiment and theory is indicated in Fig. 4, where the measured average Q_0 values and the quadrupole moments calculated for the $4^2 4^0$ configuration as a function of spin are compared with each other. The theoretical curves for the signatures $r = \pm i$ differ slightly but the present measurement is not sensitive to such a difference nor to a noticeable reduction of Q_0 at very high spin.

In conclusion, a coupled band in ^{57}Co (two signatures) has been found and the mass 60 region of deformation has been extended below the $Z = 28$ shell gap. The new structure in ^{57}Co is well described as a $4^2 4^0$ intruder configuration and, thus, supports the picture of particle-hole excitations developed for this mass region. A deformed band is also present in ^{57}Ni . However, this structure is observed in one signature only. Similar to the case of ^{57}Co , the large quadrupole moment of the band in ^{57}Ni rules out a configuration assignment without a $N_0 = 4$ intruder.

The authors express their gratitude to the support staff at ANL for assistance in setting up the experiment. They thank D.C. Radford for making available his latest software. Discussions with C.E. Svensson are acknowledged. This work was supported by US DOE under grant no. DE-FG02-88ER-40406, contracts nos. DE-AC03-76SF00098 and W-31-109-ENG-38, and by the Swedish Natural Science Research Councils.

REFERENCES

1. C.E. Svensson *et al.*, Phys. Rev. Lett. 79 (1997) 1233.
2. C.E. Svensson *et al.*, Phys. Rev. Lett. 80 (1998) 2558.
3. D. Rudolph *et al.*, Phys. Rev. Lett. 80 (1998) 3018.
4. D. Rudolph *et al.*, Phys. Rev. Lett. 82 (1998) 3763.
5. T. Mizusaki *et al.*, Phys. Rev. C 59 (1999) R1846.
6. A.V. Afanasjev, I. Ragnarsson, and P. Ring, Phys. Rev. C 59 (1999) 3166.
7. I.Y. Lee, Nucl. Phys. A 520, 641c (1990).
8. D.G. Sarantites *et al.*, to be published.
9. D.G. Sarantites *et al.*, Nucl. Inst. Meth. A 381 (1996) 418.
10. C.E. Svensson *et al.*, Nucl. Inst. Meth. A 396 (1996) 228.
11. W. Reviol *et al.*, to be published.
12. B. Cederwall *et al.*, Nucl. Inst. Meth. A 354 (1995) 591.
13. Table of Isotopes, Eighth Edition, Vol. I (1996).
14. F.A. Lerma *et al.*, Phys. Rev. Lett. 83 (1999) 5447.
15. J.F. Ziegler, J.P. Biersack, and U. Littmark, *The Stopping and Range of Ions in Solids* (New York 1985); J.F. Ziegler, priv. comm.
16. D. Rudolph *et al.*, Eur. Phys. J. A 4 (1999) 115.
17. J. Dobaczewski, W. Satula, W. Nazarewicz, and C. Baktash, to be published.